Chemical Engineering Journal 387 (2020) 124115

Contents lists available at ScienceDirect

Chemical Engineering Journal

journal homepage: www.elsevier.com/locate/cej

Magnolol-based bio-epoxy resin with acceptable glass transition temperature, processability and flame retardancy

Yu Qi, Zhihuan Weng*, Kewen Zhang, Jinyan Wang, Shouhai Zhang, Cheng Liu, Xigao Jian

State Key Laboratory of Fine Chemicals, Liaoning High Performance Resin Engineering Research Center, Department of Polymer Science & Engineering, Dalian University of Technology, Dalian 116024, China

HIGHLIGHTS

- A bio-based intrinsic flame retardancy epoxy resin was prepared from magnolol.
- It showed high thermal stability with T_g > 250 °C and $T_{d5\%}$ > 400 °C.
- The system exhibited outstanding processability, very suitable for RTM process.
- The system presented 'Excellent' and 'Good' in Cure and Flame Retardancy Index.
- It also exhibited higher mechanical modulus and strength than DGEBA.

GRAPHICAL ABSTRACT

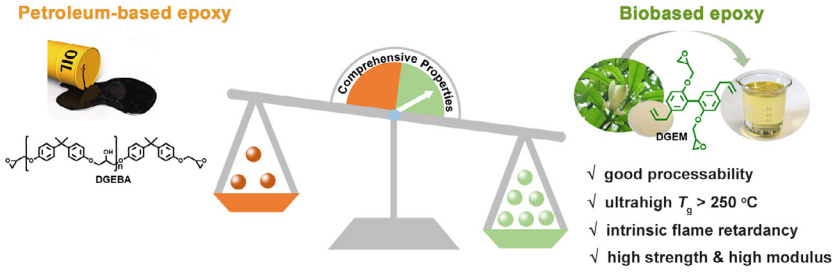

ARTICLE INFO

Keywords:
Magnolol
Biomass
Epoxy resin
Intrinsic flame retardancy
High performance

ABSTRACT

Development of sustainable bio-based epoxy resins having better comprehensive properties than available petroleum-based epoxy resins is of paramount importance for alleviation of energy pressure and enrichment of the potent category of high-performance epoxy resins. In this study, a fully bio-based epoxy resin precursor (DGEM) was synthesized from a naturally occurring magnolol through a highly efficient one step process. The bio-based epoxy resin obtained was then cured with 4, 4′-diaminodiphenyl sulfone (DDS) and compared to the petroleum-based commercial diglycidylether of bisphenol A (DGEBA). After curing with DDS, DGEM/DDS showed higher glass transition temperature than DGEBA/DDS which was 279 °C and 231 °C, respectively. The char yield (in N_2), storage modulus and flexural modulus of the former were 1.9-fold, 47.5%, and 41.3% higher than those of the latter, respectively. Interestingly, bio-based epoxy resin of DGEM exhibited excellent processability with extremely low viscosity of 0.155 Pa·s at room temperature and a broader processing window than DGEBA/DDS as well. To exhibit such an excellent processability is very rare for high-performance epoxy resins. In addition, the cured DGEM/DDS also showed outstanding intrinsic flame retardancy, which passed the V-0 rate of UL-94 test. This study offers an opportunity to prepare bio-based epoxy resins with better properties than DGEBA and exhibits great promise in cutting-edge applications.

1. Introduction

Petroleum resources have played an important role in the progress of human society and are considered as indispensable in modern life, but it is a serious issue that they are limited. The increasing consumption of the petroleum resources in modern life has caused these resources to be exhausted and caused climate changes as well as severe environmental pollution. Thus, development of renewable biomass

* Corresponding author.
E-mail address: zweng@dlut.edu.cn (Z. Weng).

https://doi.org/10.1016/j.cej.2020.124115
Received 12 August 2019; Received in revised form 5 January 2020; Accepted 11 January 2020
Available online 13 January 2020
1385-8947/

resources is an efficient and necessary solution, which can replace the petroleum resources especially in polymer area to alleviate energy and environmental pressure [1].

Epoxy resins, as one of the most important polymers, have been widely used in numerous fields such as coatings, adhesives, high-performance composites, electronic encapsulants, and so forth, because of their excellent properties of adhesion, mechanical, processability, and electrical insulation [2–4]. On the other hand, it is very unfortunate that almost all of the commercially accessible epoxy resins are synthesized from non-renewable resources like petroleum, of which more than 90% of epoxy resins are made up of diglycidyl ether of bisphenol A (DGEBA) [4]. The two main reactants of DGEBA are bisphenol A (BPA) and epichlorohydrin. Epichlorohydrin can be commercially produced using bio-based glycerol [5], while BPA can only be produced from petroleum resources, which account for more than 67% of the total molar mass for DGEBA [6]. Moreover, BPA is also an endocrine disruptor and has been classified as a reprotoxic R2 substance, which could bring great threat to human health [7,8]. Based on the above energy and health concerns, there is a growing interest in the development of sustainable and nontoxic biomass resources for preparation of bio-based epoxy resins instead of BPA. Until now, lots of work has been done on the synthesis of bio-based epoxy resins, but their comprehensive properties are not comparable with DGEBA. Most of the bio-based monomers contain long flexible aliphatic chains or alicyclic structures such as various vegetable oils [9], cardanol [10,11] and isosorbide [12,13], etc. These groups can alleviate the thermal stability and mechanical properties of the corresponding bio-based epoxy resins significantly. There are also many rigid bio-based monomers, which contain aromatic structures such as vanillin [14,15], salicylic acid [16], eugenol [17,18], etc. When they are used to synthesize epoxy resins, the glass transition temperature and mechanical properties of the corresponding bio-based epoxy resins are effectively enhanced. For instance, Wang et al. [19] synthesized a mono-functional epoxy precursor based on vanillin. When it was cured with 4,4′-methylenebiscyclohexanamine, a Schiff based epoxy thermoset was obtained, which showed similar T_g of 173 °C as compared to DGEBA. Xu et al.[20] also used vanillin for the synthesis of a Schiff base epoxy thermoset, whose T_g, tensile modulus and tensile strength were 196 °C, 2196 MPa and 93 MPa, respectively, which were all higher than those of DGEBA. Even though, further development is still needed in bio-based epoxy resin having higher T_g and mechanical properties. In order to further enhance the properties of bio-based epoxy resins, some rigid petroleum-based monomers, which include terephthaloyl chloride [21], α,α'-dichloro-p-xylene [22], p-phenylenediamine [3], etc., are introduced. However, these compounds may decrease the bio-based content and their high melting temperature may bring some difficulties in processing. Actually, polymers, which have high thermal and mechanical properties as well as good processability have always been a dilemma [23]. Therefore, development of new bio-based epoxy resins, which have comprised better properties and simpler processing than DGEBA is still a huge challenge.

Another drawback of epoxy resins is their high flammability, which have limited their applications in electronics, aerospace, and other cutting-edge areas, where flame retardancy is required [24]. Introduction of halogen elements can remarkably decrease the flammability of epoxy resins. However, these systems release highly toxic gases during the combustion process, which conflicts with sustainable and green chemistry regulations [25]. Other retardant elements and additives such as phosphorus [26], silicon [27], layered double hydroxides [28], grapheme [29] are more environmental friendly and have shown satisfactory flame retardancy effects, but they exploit poor compatibility with the matrix resins and can deteriorate the glass transition temperature and mechanical properties of the systems [30]. Development of epoxy resins with intrinsic flame retardancy without sacrificing other properties is an important strategy to extend the applications of epoxy resins in various fields, but very few studies have been done so far in this regard, especially for bio-based epoxy resins [31].

On the basis of the above evidences from literature, we concluded that the development of such a bio-based epoxy resins is much needed which can surpass DGEBA, and provide better thermal stability, good mechanical properties and excellent flame retardancy without sacrificing the processability. One of the most effective solutions is designing suitable bio-based platform monomers. Recently, a pyridazine-based compound was synthesized from bio-based guaiacol and succinic anhydride by our group, where the epoxy-resin, based on this aromatic N-heterocycle showed better comprehensive properties than DGEBA [32]. Magnolol is a kind of bioactive compound, which is extracted from the bark of magnolia officinalis. It is usually used as herbal medicine and in cosmetics and has been demonstrated as a safe compound, which shows few adverse effects [33,34]. Moreover, it is also a fascinating and multifunctional bio-based monomer and inherently contains a symmetrical bisphenol and diallyl, which is very suitable for synthesis of various bio-based polymers. Allyl is an active group, which has been widely introduced into various polymers for increasing their crosslink density and improvement of processability [23,35]. Moreover, the biphenyl structure in magnolol belongs to a group of a highly aromatic compound, when incorporated in polymers not only enhances the thermal stability but also forms a highly pyrolysis-resistant carbonaceous during combustion, thus, improving the flame retardancy of polymers [36,37]. The bisphenols in magnolol facilitate the preparation of bio-based epoxy resins. Whereas, until now, there are no literature evidences, which have shown the uses of magnolol as a raw material for production of bio-based epoxy resins.

In this study, a full bio-based epoxy precursor of DGEM was prepared through a highly efficient one step process in which magnolol and epichlorohydrin were used as raw materials. The DGEM obtained was then cured with 4,4′-diaminodiphenyl sulfone (DDS) and compared to the commercial petroleum counterpart of DGEBA. The cured bio-based epoxy resin showed better properties than DGEBA/DDS, which included their higher thermal stability, better mechanical properties, flame retardancy and better processability. Furthermore, the highest glass transition temperature was observed for this system among all other reported bio-based epoxy resins to the best of our knowledge. Our study provides an opportunity for preparation of high-performance bio-based epoxy resin which can be substituted with DGEBA.

2. Experimental section

2.1. Materials

Magnolol and benzyltriethylammonium chloride was supplied by Saen chemical technology Co., Ltd., Shanghai, China. Epichlorohydrin was purchased from Aladdin-reagent Co., Ltd., Shanghai, China. 4,4′-diaminodiphenyl sulfone was obtained from Macklin biochemical Co., Ltd., Shanghai, China. Sodium hydroxide and sodium sulfate anhydrous was obtained from Damao chemical reagent factory, Tianjin, China. Epoxy resin (DGEBA, trade name E51, epoxy value 0.51 mol/100 g) was supplied by Nantong Xingchen synthetic materials Co., Ltd, China. All chemicals were used directly without further purification.

2.2. Synthesis of diglycidyl ether of magnolol (DGEM)

Magnolol (27.96 g, 105 mmol), epichlorohydrin (485.73 g, 5.25 mol) and benzyltriethylammonium chloride (BTEAC, 2.39 g, 10.5 mmol) as the catalyst were added successively to the three-necked round-bottomed flask. The mixture was vigorously stirred at 80 °C for 3 h under nitrogen atmosphere. Afterwards, 40 %w/w aqueous sodium hydroxide (10.5 g, 262.5 mmol) was added dropwise to the reaction system and stirred for another 1 h at 80 °C. After completion of the reaction, the mixture was filtered to remove the generated salt, then the filtrate was poured into the separatory funnel, and washed several times with distilled water. After that, the combined organic layer was

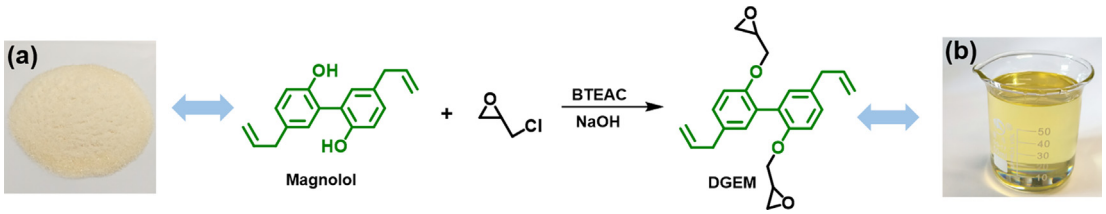

Fig. 1. Synthetic route of DGEM. (a) and (b) are the photographs of magnolol and DGEM.

separated and dried with anhydrous Na_2SO_4 overnight. Followed by concentration of the dried organic layer under vacuum to remove excess epichlorohydrin and dried at 50 °C for 24 h in a vacuum oven to obtain the target product DGEM as yellow liquid (35.37 g, yield 89%). ^{1}H NMR (500 MHz, $CDCl_3$, ppm): δ = 7.13–7.08 (m, 2H), 6.90 (d, 1H), 5.99 (ddt, 1H), 5.08 (ddd, 2H), 4.17 (dt, 1H), 3.97–3.90 (m, 1H), 3.37 (d, 2H), 3.22–3.16 (m, 1H), 2.77–2.71 (m, 1H), 2.58 (ddd, 1H). ^{13}C NMR (101 MHz, $CDCl_3$, ppm): δ = 154.47, 137.81, 132.51, 131.84, 128.47, 128.25, 115.58, 112.85, 69.35, 50.39, 44.52, 39.43. FT-IR (ATR, cm^{-1}): 1637 (C═C), 995 (═C−H), 914(═C−H and epoxy).

2.3. Thermal curing of epoxy resin

The common high-temperature curing agent 4,4′-diaminodiphenyl sulfone (DDS), was employed in this system. Firstly, DDS was added into DGEM according to the stoichiometry ratios (the molar ration of epoxy groups to N–H was 1:1). The system was stirred vigorously at 120 °C until DDS dissolved into the system completely to get a homogenous mixture. Then the mixture was degassed in a vacuum oven at 120 °C to remove the entrapped air. After that, the gas free mixture was poured into a preheated stainless steel mould and cured at 135 °C for 2 h, 180 °C for 2 h, 210 °C for 2 h, 230 °C for 2 h and 250 °C for 2 h in a muffle furnace to get a completely cured resin, named as DGEM/DDS. For comparison, DGEBA with DDS was cured at the same procedure to obtain the cured DGEBA/DDS resin.

2.4. Characterization

^{1}H NMR and ^{13}C NMR spectra were performed on the Bruker AdvanceIII500 MHz nuclear magnetic resonance spectrometer at room temperature using deuteron chloroform ($CDCl_3$) as solvent and tetramethylsilane as the internal standard. Fourier transform infrared (FT-IR) spectra were performed on a Thermo Nicolet Nexus 470 FT-IR spectrometer through attenuated total reflectance (ATR) method with the wavelength range of 650–4000 cm^{-1}. Electrospray ionization mass spectrometry (ESI-MS) was performed on a LTQ Orbitrap XL mass spectrometer with an ESI positive ion mode. The curing behaviors of the epoxy resin systems were investigated on a Mettler DSC 1 differential scanning calorimeter under a nitrogen atmosphere with the flow rate of 50 mL/min. Thermal gravimetric analysis (TGA) was carried out on a Mettler TGA 1 instrument with a heating rate of 20 °C/min. Dynamic mechanical analysis was studied through a Mettler DMA/SDTA861e dynamic mechanical analyzer in a single cantilever mode. All the samples with the dimensions of 35 mm × 5.3 mm × 3.0 mm, heating rate of 3 °C/min and frequency of 1 Hz.

Flexural properties were tested according to Chinese standard GB/T 9341–2000, performed on a WSM-50KN electric universal testing machine with the crosshead rates of 2 mm/min. The dimension of each test specimen was 80 mm × 10 mm × 4 mm, and the results were averaged from at least five measurements. Viscosity and dynamic rheological behavior of the epoxy resin systems were both investigated on a TA AR2000 rheometer, using a 25 mm diameter parallel plate geometry with 1000 um gap. Viscosity of epoxy resins were measured under steady state flow mode with the shear rates from 1 to 100 s^{-1} at 25 °C. The dynamic rheological behaviors of the epoxy resin systems were conducted under a dynamic oscillation mode. The temperature range was 25–250 °C, with a heating rate of 3 °C/min, under a frequency of 1 Hz and a stress of 10 Pa. Microscale combustion calorimeter (MCC) was carried according to ASTM D7309-13 on a FTT0001 microscale combustion calorimeter (UK). About 5 mg samples were heated from 70 −700 °C at a heating rate of 1 °C/s, under a nitrogen flow of 80 cm^3/min. Then the obtained volatile products were mixed with a stream flow of 20 cm^3/min including 80% nitrogen and 20% oxygen prior to being put into a 900 °C combustion furnace. Vertical burning test (UL-94 test) was performed according to ASTM D3801-10 on a M607B type instrument. The sample dimensions were 125 mm × 13 mm × 3 mm. The morphology of the char residues after UL-94 test was observed through scanning electron microscopy (SEM) on a FEI QUANTA 450 SEM instruments. Each specimen was sputter coated with gold before testing. X-ray photoelectron spectroscopy (XPS) was recorded on an ESCALAB 250 apparatus with an Al Kα X-ray source under a base pressure of 1 × 10^{-9} mbar. Raman spectra were carried on a RENISHAW inVia Ram Microscope. Thermogravimetric analyses-infrared spectra (TG-IR) were conducted on STA 409 PC/PG (NETZSH, Germany). About 15 mg of each sample was enclosed in an alumina crucible, and heated from 40 to 800 °C, with a heating rated of 10 °C/min under an argon atmosphere. Pyrolysis-gas chromatography/mass spectrometry (Py-GC/MS) was performed on a CDS 5200 pyrolyzer combined with an Agilent 7890/5975 GC/MS. The cracker temperature was set at 500 °C and held on 20 s under helium atmosphere.

3. Results and discussion

3.1. Synthesis and characterization of DGEM

The process of synthesis for DGEM involved an easy and highly efficient one step process. As shown in Fig. 1, DGEM was obtained through a glycidylation reaction of magnolol with excess of epichlorohydrin (which was produced via bio-based glycerol chlorination [5]) in alkaline conditions in which BTEAC was used as a phase transfer catalyst. The product obtained was purified easily without column chromatography. Moreover, the yield of the product obtained was as high as 89%, which showed that this method had a great potential for production on industrial scale. The structure of the DGEM obtained was well characterized by various methods as shown in Fig. 2 and Figs. S1 and S2. The FT-IR spectrum of DGEM (Fig. 2(b)) showed characteristic absorptions at 1637 cm^{-1} and 3075 cm^{-1} which were attributed to the stretching vibrations of −C═CH_2 and ═C−H, respectively [23]. Additionally, the characteristic bands which were shown at 995 cm^{-1} and 914 cm^{-1} were due to the out of plane bending vibration of olefin [38]. These findings suggested that allyl groups could be presented in DGEM. In the FT-IR spectrum of magnolol, the broad peaks around 3160 cm^{-1} were attributed to the stretching vibration of –OH. This peak was disappeared in the spectrum of DGEM, which indicated that the hydroxyl group had been completely glycidylated. Although, the characteristic peaks of epoxy were overlapped with the olefin peak at 914 cm^{-1} in the DGEM spectrum, it could be predicted that the epoxy group had been successfully introduced. Furthermore, the characteristic peaks of protons at 2.58 ppm, 2.73 ppm and 3.19 ppm in the ^{1}H NMR spectrum also confirmed that the epoxy group was produced. In addition, the

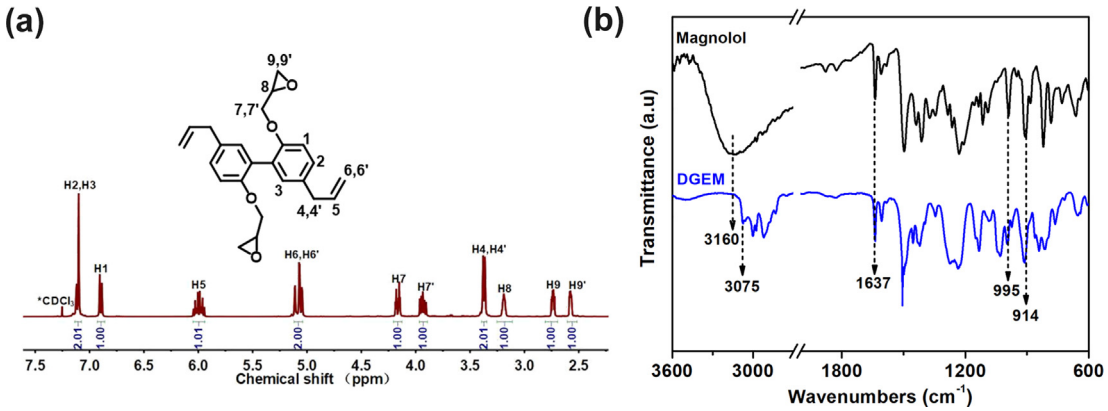

Fig. 2. Structure characterization of DGEM. (a) ^{1}H NMR spectrum of DGEM; (b) FT-IR spectra of magnolol and DGEM.

chemical shifts and integral area of all the mentioned peaks were in excellent agreement with the target product. Moreover, the ^{13}C NMR spectrum, as shown in Fig. S1, showed that the carbon resonances were well-matched with the expected structure. The ESI-MS, which is shown in Fig. S2 also confirmed that DGEM had the designed molecular weight of 378.47 (experimental results $[M+NH_4^+]$ = 396.25, $[M+Na^+]$ = 401.24), and the epoxy value of DGEM was titrated to be 0.51 mol/100 g according to the ASTM D 1652, which was very close to the theoretical epoxy value of 0.53 mol/100 g. From all the above results, it was concluded that the bio-based epoxy resin precursor of DGEM was successfully synthesized having a precise structure.

3.2. Curing behavior of DGEM/DDS

DGEM possessed interesting structural characteristics having two kinds of active functional groups. The epoxy groups in DGEM could form polymerization of epoxy ring opening with DDS. Besides this, the allyl groups in DGEM were also active groups and could handle high-temperature thermal addition polymerization. Therefore, it was hypothesized that DGEM/DDS might show some special curing behaviors, which urged further studies on the curing behaviors of DGEM/DDS. First, non-isothermal DSC test was conducted to analyze the curing behavior of DGEM/DDS. For comparison, DGEBA/DDS was also analyzed under same conditions. The corresponding DSC curves are presented in Fig. 3(a-b). Similar to DGEBA/DDS, the DSC curves of DGEM/DDS also showed only one exothermic peak. As reported in many studies [39–41], usually the allyl groups could recognize thermal addition polymerization at 170–250 °C, which fell exactly within the temperature range of opening reaction of amine-epoxy ring. Therefore, the widened exothermic peak of DGEM/DDS may be attributed to the superposition of the amine-epoxy ring opening reaction and allyl addition polymerization. The key data of non-isothermal DSC tests (summarized in Table S1) was used to calculate the Cure Index (CI), which is a simple criterion to evaluate qualitatively the crosslinked situation of thermoset systems [42]. The CI equation and detailed calculations were elucidated in Eq. (S1) and Table S1. After calculations, the CI value of DGEBA/DDS revealed that its curing state was “Excellent Cure”. Then the curing activation energy of the two resin systems were calculated according to isoconversional Kissinger-Akahira-Sunose (KAS) methods [43], which are provided in Eq. (S2). As shown in Fig. S3(a) and (b), both DGEM/DDS and DGEBA/DDS showed sigmoidal shapes in the plots of conversion versus temperature curves, which suggested that both the systems showed autocatalytic behavior during the process of curing. The activation energy (E_a) versus conversation curves obtained are shown in Fig. 3(c). The average E_a for DGEM/DDS and DGEBA/DDS were calculated to be 64.5 kJ/mol and 69.1 kJ/mol, respectively. The lower E_a of DGEM/DDS indicated that it had higher curing reactivity than that of DGEBA/DDS. This higher curing reactivity was attributed to the presence of allyl groups in DGEM, which led to improve the motion of molecules and enhanced the collisions probability of the epoxy groups and curing agent. Moreover, as reported in the literature, additional polymerization of allyl groups could produce active hydrogen [44], which promoted the epoxy ring-opening polymerization. Therefore, it was concluded that DGEM/DDS showed higher curing reactivity.

In order to study the curing reaction of DGEM/DDS further, FT-IR was carried out. Fig. 3(d) represents the FT-IR spectra of DGEM/DDS at different curing stages. The IR characteristic bands attributed to the allyl groups at 1637 cm^{-1}, 955 cm^{-1} and 914 cm^{-1} (the band at 914 cm^{-1} was overlapped with epoxy groups) started decreasing gradually with increase in the curing stages and almost disappeared completely in the final curing stage. These findings demonstrated that the allyl groups in DGEM/DDS could be polymerized when the temperature got inclined. It also suggested that post-curing temperature of 250 °C was required for DGEM/DDS systems to guarantee the complete curing of the allyl groups. Thus, after the final curing stages, the systems realized sufficient curing. According to the FT-IR results, it was concluded that the DGEM/DDS system mainly contained two types of reactions during the curing process. The first type of reactions was the reaction of the amine-epoxy ring opening, which are shown in Fig. 4 (a). First, the primary amine opened the epoxy ring, which formed a secondary amine and an alkanol. Then the secondary amine obtained reacted with another epoxy ring and formed a tertiary amine and an alkanol. The second type of reaction was allyl thermal addition polymerization reaction (Fig. 4(b)). The allyls in DGEM recognized the addition polymerization at high temperature, which finally formed the polyolefin structure. After the final curing stage as mentioned in FT-IR test, the above two types of reaction reacted almost completely and formed a highly cross-linked network as shown in Fig. 4 (II).

3.3. Thermomechanical and mechanical properties of the cured resins

In terms of the DSC and FT-IR results, the two curing conditions for DGEM/DDS were applied which were 135 °C, 2 h + 180 °C, 2 h + 230 °C, 2 h, and 135 °C, 2 h + 180 °C, 2 h + 210 °C, 2 h + 230 °C, 2 h + 250 °C, 2 h. DGEM/DDS was cured according to the above conditions and named as DGEM/DDS-1 and DGEM/DDS-2, respectively. For comparison, DGEBA/DDS was also cured under the same conditions which were applied to DGEM/DDS-2. The thermomechanical properties of these cured resins were characterized by DMA, which is shown in Fig. 5(a). DGEM/DDS-1 showed two tanδ peaks, in which the main peak was attributed to its T_g at 172 °C. The small and weak peak might be resulted due to the insufficient curing of the system. According to the FT-IR results, which are shown in Fig. 3(d), it was suggested that in the cured DGEM/DDS-1, unreacted allyl groups and some residual epoxy groups were still here. As reported in a previous study [40], the addition polymerization of allyl groups

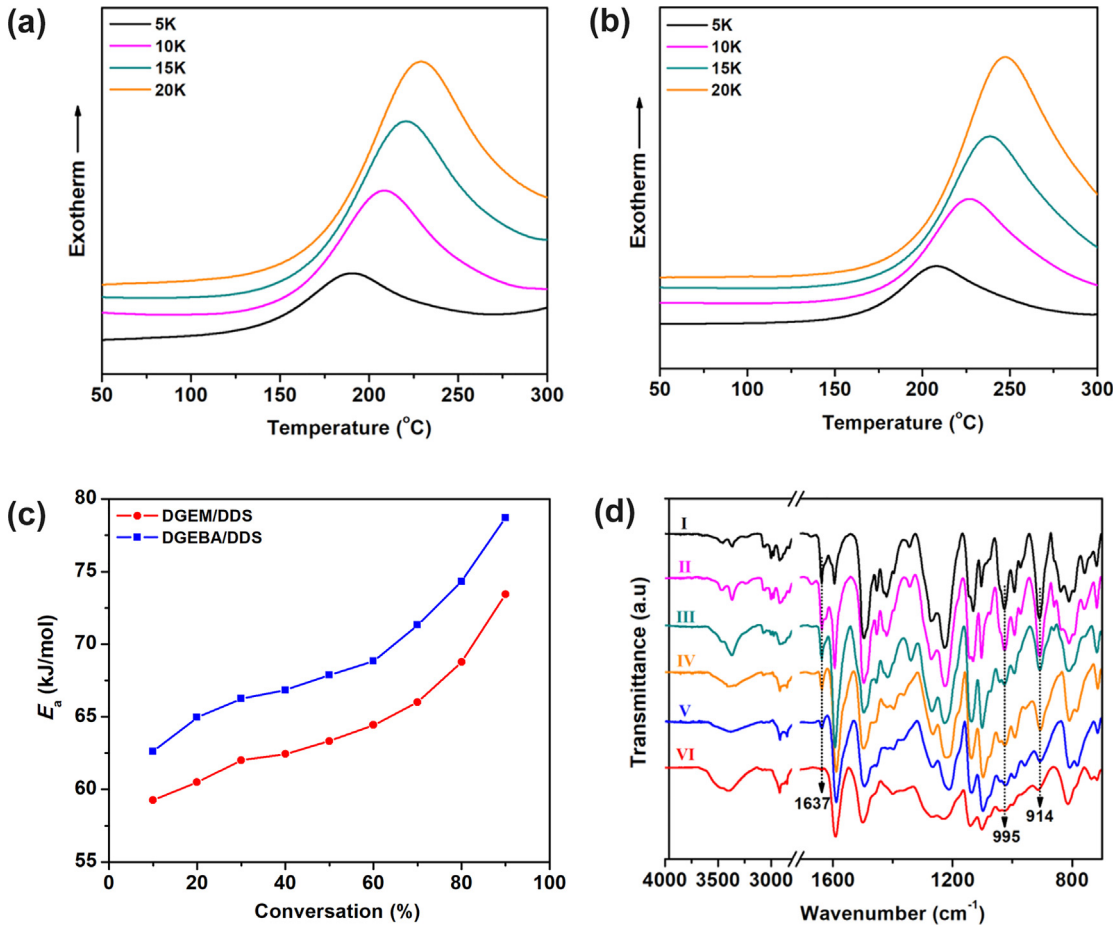

Fig. 3. Curing behavior of DGEM/DDS and DGEBA/DDS. (a) Non-isothermal DSC thermographs of DGEM/DDS with various heating rates. (b) Non-isothermal DSC thermographs of DGEBA/DDS with various heating rates. (c) Activation energy versus conversion curves for DGEM/DDS and DGEBA/DDS. (d) FT-IR spectra for DGEM/DDS system at different curing stages. I: uncured; II: 135 °C for 2 h;III: 135 °C for 2 h and 180 °C for 2 h; V: 135 °C for 2 h, 180 °C for 2 h and 210 °C for 2 h;VI: 135 °C for 2 h, 180 °C for 2 h, 210 °C for 2 h and 230 °C for 2 h;VII: 135 °C for 2 h, 180 °C for 2 h, 210 °C for 2 h, 230 °C for 2 h and 250 °C for 2 h.

was a slow process, which needed high temperature and long duration. Therefore, the curing condition which was used for DGEM/DDS-1 was not enough for allyl groups to recognize sufficient reaction. The probable structure of the cured DGEM/DDS-1 is illustrated in Fig. 4(I). It could be seen that only partial allyl groups recognized addition polymerization, because the crosslink density of the DGEM/DDS-1 was 867 mol/m^3, which was calculated on the basis of the famous rubber elasticity theory [45,46] (explained in Eq. (S3)), which ultimately resulted in a low T_g for DGEM/DDS-1. With increase in the temperature during the DMA test, the residual allyl groups and epoxy groups continued to react and the cross-linking density of the system was further increased, which led to the appearance of another T_g at 240 °C. The DGEM/DDS-2 showed the highest T_g (279 °C) among all the three epoxy systems, which was calculated to be 48 °C higher than that of DGEBA/DDS. Generally, T_g can be determined along with the molecular chain rigidness and crosslink density of the system. The allyl groups in DGEM provided extra crosslink sites for DGEM/DDS systems. Furthermore, the allyl groups and epoxy groups in DGEM/DDS-2 were cured almost completely, which had been confirmed already by FT-IR, as shown in Fig. 3(d). The curing condition which was used for DGEM/DDS-2 took long curing duration of 10 h, and added 250 °C post curing temperature, which could accelerate the reaction further towards completion. The probable structure of the cured DGEM/DDS-2 is shown in Fig. 4(II). The allyl groups recognized sufficient polymerization which made the system to form highly cross-linked network structure. Therefore, DGEM/DDS-2 possessed considerably high crosslink density of 3176 mol/m^3, which was much higher than DGEBA/DDS (2335 mol/m^3) as shown in Table 1. On the other hand, the biphenyl moiety presented in the main chain of DGEM made the systems to have higher rigidness. All of these properties resulted in the enhancement of T_g of DGEM/DDS-2. As far as it is known, 279 °C was the highest T_g among all the previously reported bio-based epoxy resins, whose corresponding properties are compared in Fig. 7. Since the storage modulus reflects the rigidness of the systems, both the DGEM/DDS-1 and DGEM/DDS-2 showed higher storage modulus than DGEBA/DDS. These high storage modules were attributed to the diphenyl moiety in DGEM, which endowed these systems with higher rigidness. In our study, the curing condition used for DGEM/DDS-2 was chosen as the final protocol for DGEM/DDS system. All the other properties of cured DGEM/DDS studied and mentioned in the following parts of this article were based on this chosen curing protocol.

Fig. 5(b) shows the flexural properties of the cured resins, which are summarized and listed in Table 1. DGEM/DDS displayed the ultra-high flexural modulus of 3455 MPa, which was calculated to be 41.3% higher than DGEBA/DDS (2446 MPa), and could be attributed to the high rigidness and high crosslink density of DGEM/DDS systems. Moreover, the flexural strength of DGEM/DDS was also calculated to be higher than that of DGEBA/DDS (108.1 vs. 106.6 MPa). Thus, the DGEM/DDS possessed a high T_g of 279 °C, along with high strength and modulus, which proved that it has great potential in high-performance application fields.

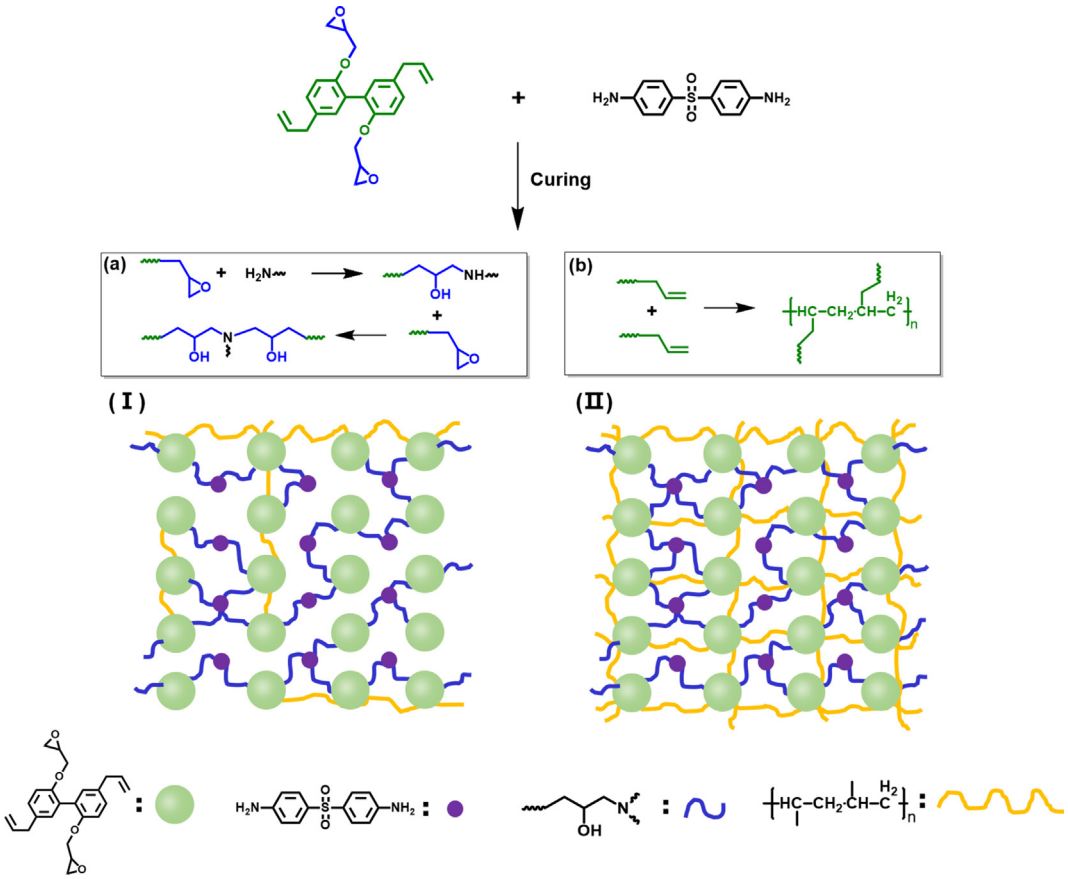

Fig. 4. Curing route of DGEM with DDS and the probable crosslinked structure of DGEM/DDS. (a) Epoxy rings opening polymerization reaction. (b) Allyl groups thermal addition polymerization reaction. (I) The probable crosslinked structure for DGEM/DDS-1. (II) The probable crosslinked structure for DGEM/DDS-2.

3.4. Thermal stability of the cured epoxy resins

Thermal stabilities of the cured DGEM/DDS and DGEBA/DDS were studied using TGA under N_2 and air atmosphere. Fig. 6 shows the corresponding TGA and derivative thermogravimetry (DTG) curves in N_2. The related curves in air and the key data are presented in Fig. S4 and Table S2, respectively. The DGEM/DDS showed extremely high thermal stability as shown in Fig. 6. In both the N_2 or air atmosphere, DGEM/DDS exhibited an ultra-high initial degradation temperature, with 5 wt% mass-loss temperature ($T_{d5\%}$) up to 402 °C, even higher than that of DGEBA (399 °C in N_2 and 395 °C in air). Until now, 402 °C is the highest $T_{d5\%}$ among all the bio-based epoxy resins reported in the literature, which has been summarized in Fig. 7 and Table S6. That is because most of the bio-based epoxy resins containing one or more labile groups such as methoxy groups [21,47,48], aliphatic bonds [49,50], ester bonds [6,51], phosphate esters [3,17], etc., which can get readily decomposed at lower temperatures. However, in the case of DGEM, there were no labile groups. Moreover, the rigid rod-like biphenyl moiety inherent in DGEM, further enhanced the thermal stability of the resin system. On the other hand, the allyl groups in DGEM got crosslinked almost completely after the process of curing, which resulted in higher crosslink density for DGEM/DDS system. According to the literature, increasing the crosslink density of the resin systems leads to enhance their initial degradation temperature [3]. Therefore, the highly crosslinked DGEM/DDS also led to enhance the $T_{d5\%}$ of this system. In N_2 atmosphere, both the DGEM/DDS and DGEBA/DDS

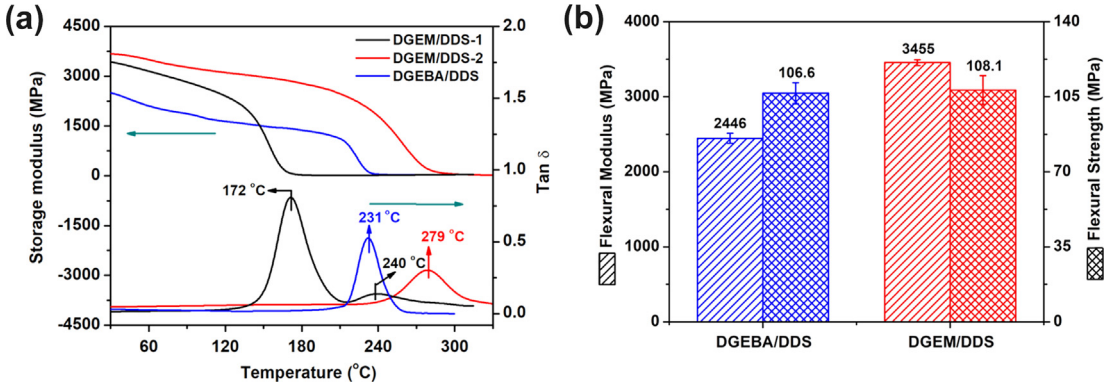

Fig. 5. Thermomechanical and mechanical properties of the cured resins. (a) DMA spectra for the storage modulus and Tanδ against temperature of DGEM/DDS-1, DGEM/DDS-2 and DGEBA/DDS. (b) Flexural properties comparison between DGEBA/DDS and DGEM/DDS.

Table 1
Comparison of properties from DMA and flexural testing for cured resins.

	T_g[a] (°C)	E' (30 °C)[b] (MPa)	V_e[c] (mol·m^{-3})	Flexural modulus (MPa)	Flexural strength (MPa)
DGEM/DDS-1	172, 240	3433	867	–	–
DGEM/DDS-2	279	3678	3176	3455 ± 39	108.1 ± 6.7
DGEBA/DDS	231	2493	2335	2446 ± 66	106.6 ± 4.9

[a] T_g: Glass transition temperature defined by the peak value temperature of tanδ against temperature curve.
[b] E' (30 °C): Storage modulus at 30 °C measured by DMA.
[c] V_e: Cross-linked density.

showed a one-step process of pyrolysis. As shown in Fig. 6(b), the maximum degradation rate of DGEM/DDS was much lower than DGEBA/DDS, with a 65% reduction. This finding indicated that the decomposition process of DGEM/DDS was more sluggish than that of DGEBA/DDS. Notably, the DGEM/DDS showed an extremely high char yield, which was calculated to be 42.8% at 700 °C, showing that it was 1.9-folds higher than that of DGEBA/DDS which was 14.6%. This high char yield of DGEM/DDS is usually very rare in the epoxy resin systems without any flame-retarding additives or elements. These findings were attributed to the presence of biphenyl structure in DGEM and higher crosslinked density of the system. The aromatic-rich structure endowed the systems with a higher char yield. In the previous studies [52,53], char residues were increased sufficiently due to introduction of the biphenyl moieties into the backbone of resin systems. The high aromaticity of biphenyl promoted the systems to form a highly pyrolysis-resistant carbonaceous during the thermal pyrolysis [36,37]. Besides the high aromaticity, enhancement of the crosslinked density of resin systems also increased their char yields [54]. The presence of allyl groups in DGEM provided extra crosslinked sites and caused DGEM/DDS systems to exhibit higher crosslinked density, which increased the char yield of the systems further.

In summary, DGEM/DDS presented an excellent thermal stability along with ultra-high $T_{d5\%}$ and high char residues. In general, the higher char yield also reflects the better flame retardancy of the resin. Because, they could serve as a protective layer which plays an important role in the inhibition of heat and oxygen transformation and protects the resin matrix from further pyrolysis. The flame retardancy of DGEM/DDS will be discussed further in this paper.

Then, T_g and $T_{d5\%}$ of DGEM/DDS were compared with other bio-based epoxy resins reported in the literature [3,6,17,20–22,47–51,55–60]. The data of this comparative analysis are presented in Fig. 7 and Table S6. The comparative analysis showed that most of the bio-based epoxy resins had T_g and $T_{d5\%}$ below 200 °C and 350 °C, respectively. The bio-based epoxy resins which have T_g above 200 °C are very rare. The DGEM/DDS system reported in this study, is therefore the first bio-based epoxy resin which simultaneously showed T_g and $T_{d5\%}$ above 250 °C and 350 °C, respectively and suggested its excellent advantage of high thermal stability.

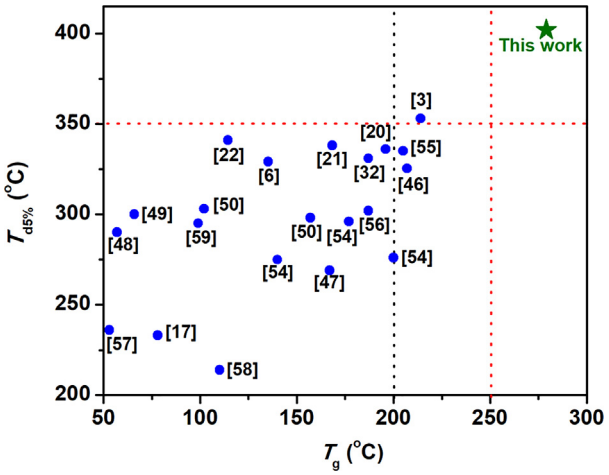

Fig. 7. Comparison of this work with other bio-based epoxy resins reported in the literature in terms of T_g and $T_{d5\%}$.

3.5. Processability of the epoxy systems

Viscosity plays an important role in determining the processability of polymers. For example, the viscosity of polymer is required to be less than 1 Pa·s during the processing window, when they are used for fiber-reinforced composites or resin transfer molding (RTM)[61]. However, in general, polymers which have excellent T_g and mechanical properties are difficult to be processed, because of the presence of rigid structures in these systems which can enhance their viscosity. For instance, the divanillin-based epoxy resin [55], DiGEDVA, exhibits high viscosity of 1300 Pa·s at 40 °C and has become difficult to be blended with any curing agent. Wan [21] reported a partial bio-based high-performance epoxy resin of TPEU-EP, which has an ultra-high melting point of 174 °C, due to its full aromatic ester structures, and encountered enormous difficulties in processing. The processability of this polymer has

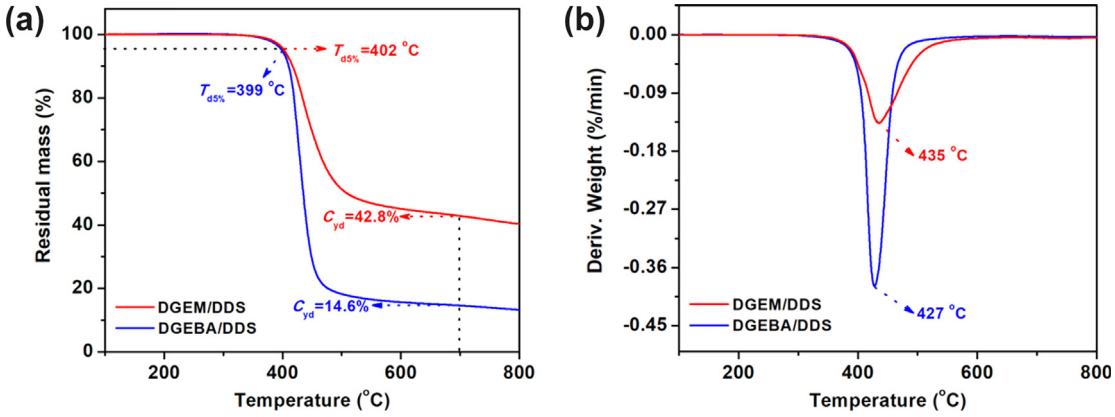

Fig. 6. Thermal stability of the cured resins. (a) TGA and (b) DTG curves of cured DGEM/DDS and DGEBA/DDS with heating rate of 20 K/min under N_2 atmosphere.

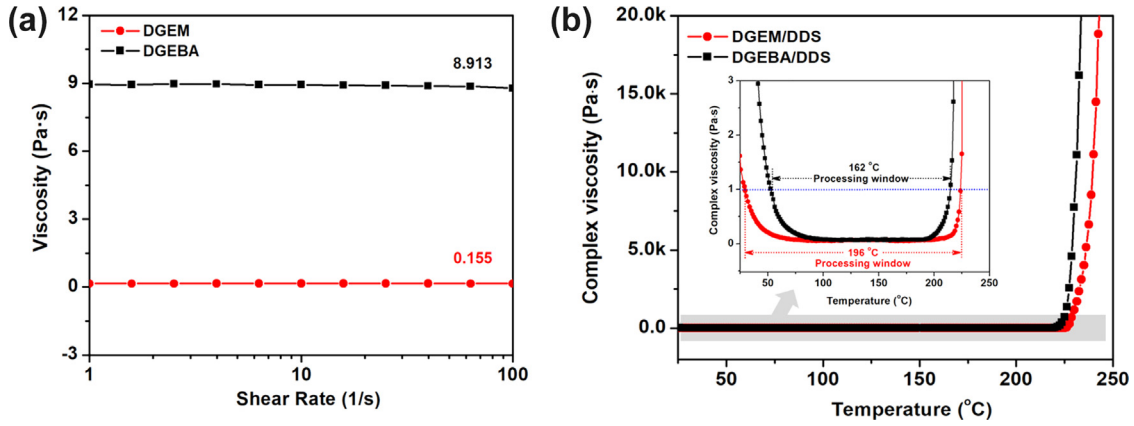

Fig. 8. Processability of epoxy resin systems. (a) Viscosity as a function of shear rate from 1 to 100 s^{-1} at 25 °C for DGEM and DGEBA without curing agents. (b) Complex viscosity as a function of temperature for DGEM/DDS and DGEBA/DDS.

not been reported yet. In contrast, DGEM in this study possessed extraordinary thermal and mechanical properties as well outstanding processability. Since DGEM was liquid at room temperature (the physical state of DGEM is shown Fig. 1(b)), the viscosities of neat DGEM and DGEBA were compared using rotational rheology approach at 25 °C. As shown in Fig. 8(a), both the resins behaved as Newtonian fluids, because their viscosities were stable during the shear rate ranging from 1 to 100 s^{-1}. Interestingly, even at 25 °C, DGEM still had an extremely low viscosity of 0.155 Pa·s, which was much lower than that of DGEBA (8.913 Pa·s). This low viscosity of DGEM was attributed to the presence of flexible allyl moieties in DGEM, which ultimately enhanced the mobility of rigid biphenyl backbone and effectively reduced the melting viscosity of the system. As reported in the literature [23,35], allyl group is a flexible aliphatic group, which has been widely applied in various resin systems in order to decrease the viscosity and broaden the processing window. Processing window is also considered an important feature of resins processing which has been evaluated efficiently by dynamic rheology. The complex viscosities of both the curing systems of DGEM/DDS and DGEBA/DDS are shown in Fig. 8(b). At 25 °C, DGEM/DDS system showed much lower viscosity than DGEBA/DDS system which was 1.5 Pa·s and 31.3 Pa·s, respectively. Furthermore, DGEM/DDS system kept viscosity below 1 Pa·s in temperature range of 29 °C to 225 °C, exhibiting a wide processing widow of 196 °C, which was even wider than that of DGEBA/DDS whose value was 162 °C. These results demonstrated that DGEM/DDS possessed a desirable processability, which was very favorable to RTM process.

3.6. Flame retardancy and the mechanism of cured epoxy resins

Microscale combustion calorimetry (MCC), which is a quantitative and rapid method, was used for comparison of the flammability of the cured DGEM/DDS and DGEBA/DDS. As illustrated in Fig. 9, the DGEM/DDS showed lower peak heat release rate (PHRR) and total heat release (THR) than that of DGEBA/DDS, which were reduced up to 70% and 26%, respectively. This reduction indicated that the DGEM/DDS released much fewer combustible substances during the process of pyrolysis, which suggested that it exhibited lower flammability than DGEBA/DDS. The obtained PHRR, THR and time-to-ignition (TTI) (summarized in Table S3) were used to calculate the Flame Retardancy Index (FRI), which is a universal dimensionless criterion for evaluation of the flame retardancy of resin systems [62,63]. The FRI was calculated according to Eq. (1).

$$FRI = \frac{\left[THR\times\left(\frac{PHRR}{TTI}\right)\right]_{DGEBA/DDS}}{\left[THR\times\left(\frac{PHRR}{TTI}\right)\right]_{DGEM/DDS}} \quad (1)$$

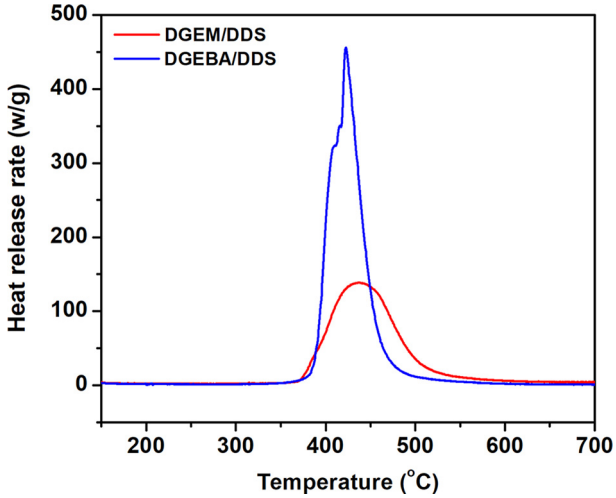

Fig. 9. Heat release rate versus temperature curves form MCC tests for cured DGEM/DDS and DGEBA/DDS.

The FRI value for DGEM/DDS system was calculated to be 4.4. According to the literature [62], the FRI values between 1 and 10 are considered as “Good” flame retardancy performance. On the basis of this, it was concluded that DGEM/DDS showed a remarkable improvement in the flame retardancy as compared to DGEBA/DDS. That was correlated to the Cure Index of DGEM/DDS, which was considered as “Excellent Cure”. The better curing state for thermoset was beneficial for enhancement of its flame retardancy. Therefore, the Cure Index for DGEM/DDS which showed “Excellent cure” was in great agreement with the Flame Retardancy Index that showed “Good” flame retardancy.

The vertical burning test (UL-94) is an efficient method for evaluation of the flame retardancy of polymer systems. In order to compare the flame behaviors of DGEM/DDS and DGEBA/DDS with more precise, the representative digital photos were taken during the combustion process, as presented in Fig. 10(a). After it was ignited in the beginning, DGEBA/DDS burned down continuously without self-extinguishing. Even after 120 s, it was still burning vigorously and a serious melt-dripping was observed, which resulted in its high flammability, and failed to qualify the UL-94 test. While in case of DGEM/DDS, it got extinguished spontaneously after ignition in the beginning in a short time duration of 2.3 s. Moreover, it again got self-extinguished about 5 s after the second ignition without any melt-dripping during the whole combustion process. These results demonstrated that DGEM/DDS had great flame retardancy and passed the V-0 rates of UL-94 tests. After these tests were analyzed, the residual test bar of DGEBA/DDS was very

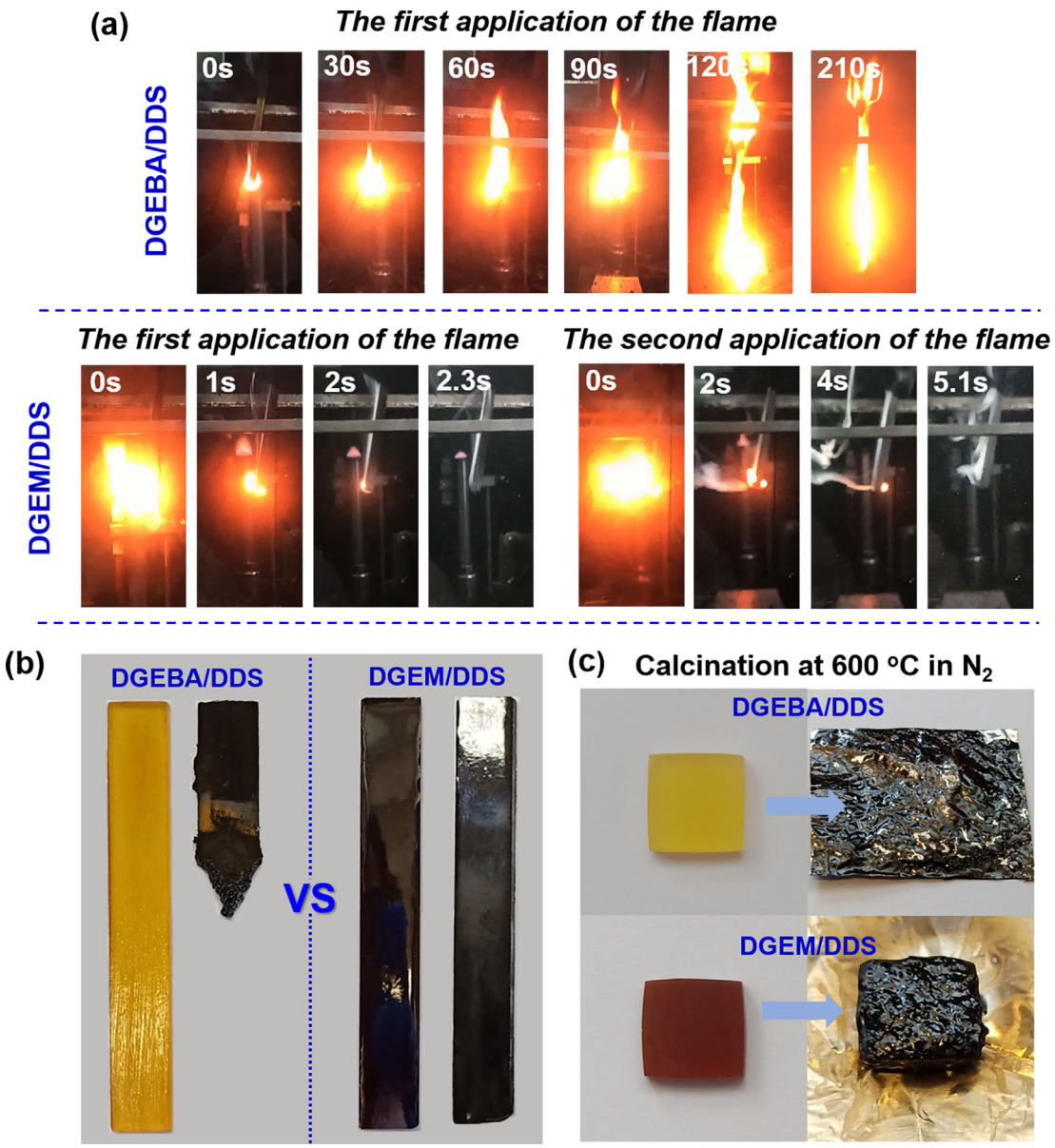

Fig. 10. Flame retardancy of DGEBA/DDS and DGEM/DDS. (a) Digital photos taken from the representative moments of UL-94 tests for DGEBA/DDS and DGEM/DDS. (b) Digital photos of UL-94 test bar before and after test for DGEBA/DDS and DGEM/DDS. (c) Digital photos of cured epoxy resins before and after calcination at 600 °C in N_2 atmosphere for DGEBA/DDS and DGEM/DDS.

short and little char residues were left on its surface due to its poor charring ability, as shown in Fig. 10(b). Whereas, the residual test bar of DGEM/DDS was still long and only a little at the bottom was burned, which was covered with compact char residues. These findings suggested that DGEM/DDS had better flame retardancy and charring ability than DGEBA/DDS.

For detailed comparison of the char residues formed from both the epoxy resin systems, the cube-like epoxy resins which comprised of 10 mm × 10 mm × 3 mm were heated from room temperature to 600 °C at a heating rate of 10 °C/min in a tube furnace under N_2 atmosphere. The morphology of the cured resins after calcination was recorded by a digital camera, which is shown in Fig. 10(c). After calcination, DGEBA/DDS showed bits of char residue with a fragmented and collapsed structure and led to inferior flame retardancy. In contrast, DGEM/DDS had retained its cubic-like structure after calcination and showed a compact and integrated charred layer having a little intumescent. These results further suggested that DGEM/DDS possessed better charring ability and more stable char layer than DGEBA/DDS, which was beneficial for enhancement of the flame retardancy.

In general, the quality of charred residues which is formed during combustion process plays an important role in determination of the flame retardancy of polymers. The mechanism of flame retardancy can be revealed by studying the physical morphology and chemical structure of the charred residues [3]. Therefore, the morphology of materials which were obtained from the UL-94 test was studied by SEM, which is illustrated in Fig. 11. When studied, the outer layer of residual chars which were collected from DGEBA/DDS (Fig. 11(a-b)) was found to be cracked, loosed and discontinuous, so they could not protect the matrix effectively. Therefore, the inner char layers (Fig. 11(c)) also possessed cracked structures, suggesting the inferior flame retardancy. However, the outer char residues of DGEM/DDS (Fig. 11(d and e)) were found to be integral, compact and continuous, which served as a high quality insulation layer and prevented the transfer of heat and gases to protect the inside matrix. Interestingly, the inner charred layer of the char residues which were collected from DGEM/DDS (Fig. 11(f)) contained a honeycomb-like cavity structure, which accumulated the pyrolytic

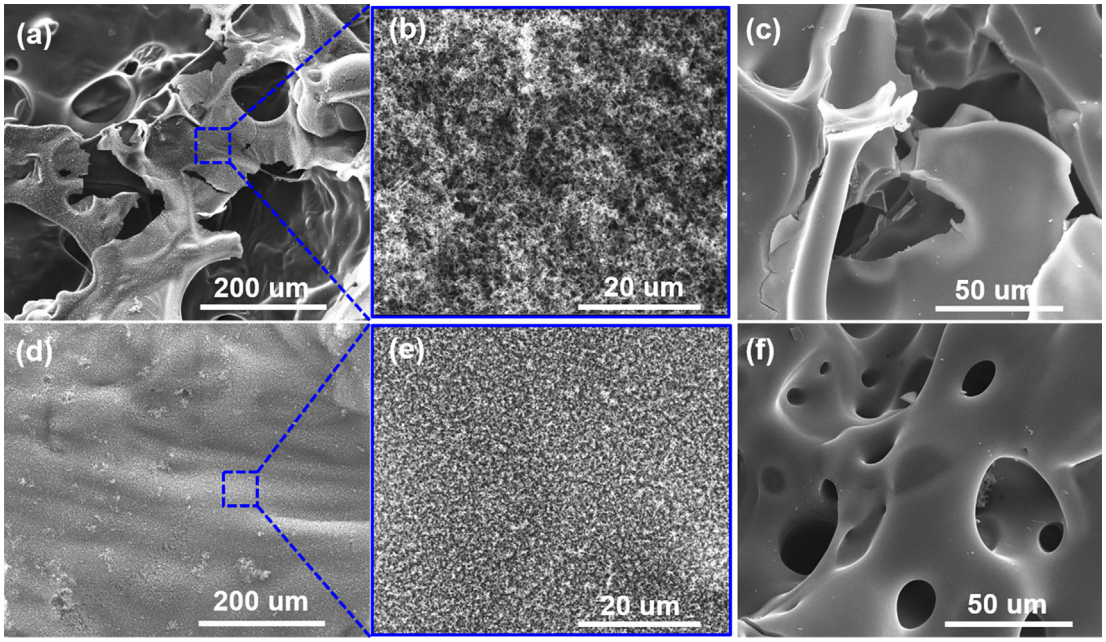

Fig. 11. SEM images of the residual chars collected from the test bars after vertical burning tests. (a, b): Outer layer of residual chars collected from DGEBA/DDS; (d, e): Outer layer of residual chars collected from DGEM/DDS. (c): Inner layer of the residual chars collected from DGEBA/DDS; (f): Inner layer of the residual chars collected from DGEM/DDS.

gases and promoted the formation of an intumescent char layer structure. Therefore, it was concluded that DGEM/DDS exhibited excellent flame retardancy and showed a condensed phase mechanism for flame retardancy.

The chemical composition and states of the char residues after UL-94 test were further analyzed by XPS. Fig. S5 and Table S4 show the corresponding XPS spectra and elemental composition, respectively. The elemental compositions of the char residues were almost the same for both the DGEM/DDS and DGEBA/DDS, while their chemical states were different. The C1s spectrum of the charred residues collected from DGEM/DDS were split into more peaks than that of DGEBA/DDS. The peaks at 284.1 eV were ascribed to C–C and C–H in aliphatic and aromatic groups, while the peaks at 285.4 eV and 291.0 eV were attributed to C-N [64] and the shake-up satellite of Π-Π* transition, respectively. The above mentioned three peaks were found in both the DGEM/DDS and DGEBA/DDS spectra. However, the peak which was centered at 286.5 eV was attributed to both the C═C and C═N [64] groups, and observed only in the C1s spectrum of DGEM/DDS. These findings suggested that more chars having steady cross-linked structures were composed of C═C and C═N, which were formed by aromatization at high temperature in DGEM/DDS system. In general, aromatic structures formed during the degradation process played a vital role in self-extinguishing and flame retardancy during the combustion process [64,65]. The N1s spectrum of DGEBA/DDS were split into pyrrole nitrogen and oxidized nitrogen, which was centered at 399.0 eV and 405.8 eV, respectively, as shown in Fig. S5(b). In case of DGEM/DDS, besides these peaks, the N1s were split into another peak as well, which was centered at 398.1 eV and attributed to pyridine nitrogen [66]. It was considered to be more thermally stable, and have benefits to form more stable carbon layer [67,68]. These findings indicated that the char residues of DGEM/DDS contained more stable structures than that of DGEBA/DDS, which further confirmed that the char residue of DGEM/DDS is much more stable and stronger than that of DGEBA/DDS, beneficial to protect the matrix and enhance the flame retardancy of DGEM/DDS.

Raman spectroscopy has also been used as an effective method to investigate the structures of the carbonaceous materials. The external chars of DGEM/DDS and DGEBA/DDS after UL-94 tests were characterized by Raman spectroscopy (as shown in Fig. S6). Both the samples exhibited two peaks at 1360 cm^{-1} (D bond) and 1600 cm^{-1} (G bond), which indicated the presence of the disordered graphite or glassy carbons and ordered graphite carbons, respectively. In general, the graphitization degree of the char residues is calculated by the ratio of integral intensities of the D and G bonds (I_D/I_G). The lower value of I_D/I_G indicates the higher graphitization degree of the char residues [69]. As shown in Fig. S6, the I_D/I_G ratio of DGEM/DDS was calculated to be 2.58, which was lower than that of DGEBA/DDS (2.95). This demonstrated that the char residues in DGEM/DDS exhibited more graphitic structures than that of DGEBA/DDS, which was also beneficial for DGEM/DDS to form stable and compact char layers.

For further understanding of the flame retardancy mechanism, TG-IR technology was used, which monitored the pyrolysis components in the gaseous phase directly. Fig. S7 shows the total absorbance of the gas-phase products for both the resin systems. Both the resins had similar weights, therefore, intensities of the absorbance peaks directly reflected the amount of the pyrolysis products [56]. It can be seen from Fig. S7 that the DGEM/DDS had lower absorbance peak intensities than DGEBA/DDS, which indicated that the cured DGEM/DDS resin released fewer pyrolysis products than DGEBA/DDS. Fig. 12(a) and (b) shows the FT-IR spectra of the products volatilized from DGEM/DDS and DGEBA/DDS at their respective pyrolysis temperatures during the TG-IR test. In Fig. 12 (b), the major absorption peaks observed at the initial pyrolysis temperature of 399 °C for DGEBA/DDS were attributed to various hydrocarbons (3185–2800 cm^{-1}), CO_2 (2390–2260 cm^{-1}, 670 cm^{-1}), CO (2188–2035 cm^{-1}), carbonyl compounds (1755 cm^{-1}), aromatic ring compounds (1510 cm^{-1}), SO_2 (1342 cm^{-1}) and Ar-N (1310 cm^{-1}) [70,71]. When the temperature was increased to the maximum pyrolysis temperature of 427 °C for DGEBA/DDS, additional pyrolysis products, such as aromatic compounds (1603 cm^{-1}, 1510 cm^{-1}), Ar-O (1260 cm^{-1}), phenolic compounds (3654 cm^{-1}) and aliphatic ethers (1179 cm^{-1}, 1098 cm^{-1}) were detected. The absorbance peak intensities of these pyrolysis compounds were increased when the temperature was increased to 450 °C. This observation demonstrated that the backbone of DGEBA/DDS system broke down during the pyrolysis process and lots of aromatic structures were escaped from the system, which accounted for its poor charring ability.

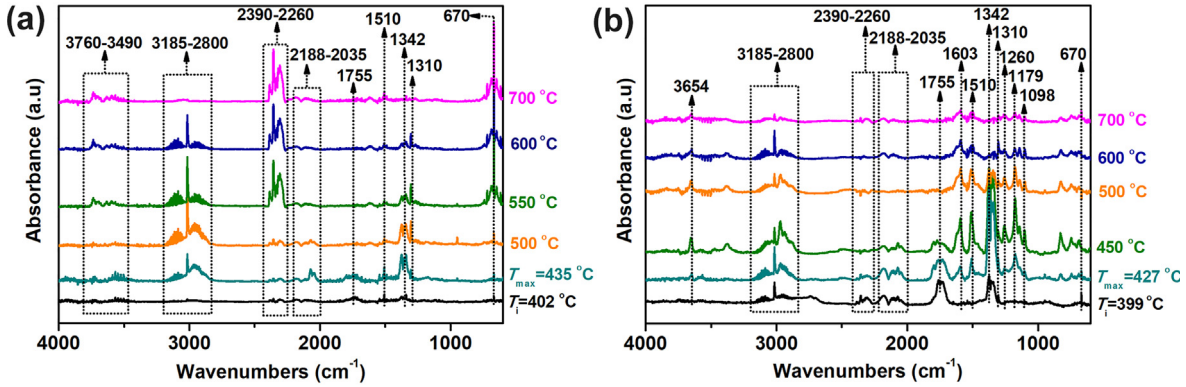

Fig. 12. TG-IR test results of DGEBA/DDS and DGEM/DDS. (a) FT-IR spectra of the pyrolysis products for DGEM/DDS system at the representative pyrolysis temperature; (b) FT-IR spectra of the pyrolysis products for DGEBA/DDS system at the representative pyrolysis temperature.

These aromatic and ether compounds were sustained released until 700 °C. At 700 °C, the absorbance peaks intensities of these compounds got weakened, which suggested the complete pyrolysis of the DGEBA/DDS system. In case of DGEM/DDS as shown in Fig. 12(a), some similar pyrolysis products were detected at 402–500 °C, such as hydrocarbons (3185–2800 cm^{-1}), CO_2 (2390–2260 cm^{-1}, 670 cm^{-1}), CO (2188–2035 cm^{-1}), carbonyl compounds (1755 cm^{-1}), aromatic ring compounds (1510 cm^{-1}), SO_2 (1342 cm^{-1}) and Ar-N (1310 cm^{-1}). However, the absorbance peaks of the flammable carbonyl compounds were much weaker than those in DGEBA/DDS system, which indicated that the DGEM/DDS systems released fewer flammable carbonyl components, which resulted in reduction of the flammable fuels supply and enhancement of its flame retardancy. On the other hand, only trace aromatic products were detected in the DGEM/DDS system, which indicated that most of the aromatic structures remained in the condensed phase during the process of pyrolysis and formed stable rich aromatic char layer, which further enhanced the flame retardancy. When the temperature was increased to 550 °C, the absorbance peak of CO_2 was observed to be enhanced clearly. While, at 700 °C, almost no other pyrolysis products were detected except CO_2 and H_2O (3760–3490 cm^{-1}). These observations suggested that the aromatic carbonaceous layer was formed during this temperature range through dehydration, decarboxylation and aromatization [72]. A large number of nonflammable CO_2 took away the heat and diluted the concentration of oxygen and other flammable gases, which enhanced the flame retardancy of this system.

To understand the charring mechanism and its contribution to the flame retardancy of the DGEM/DDS system, the Py-GC/MS test was performed. Fig. 13 shows the total ion chromatograms of both the DGEM/DDS and DGEBA/DDS systems while the products assigned to these chromatograms listed in Table S5. In case of the DGEBA/DDS, the major pyrolysis components were numerous aromatic compounds, such as styrene (peak 3′), phenol (peak 5′), phenol, 4-(1-methylethyl)- (peak 9′) and phenol, 4-(1-methylethenyl)- (peak 10′). All these components were produced from the pyrolysis process of the bisphenol A fragments, which were presented in the backbone of DGEBA/DDS. Other products, which were observed were benzenamine (peak 4′), benzenamine, N-methyl- (peak 6′), benzenamine, N, N-dimethyl- (peak 7′), which were produced during the pyrolysis process of the 4, 4′-diaminodiphenyl sulfone fragments. On the basis of these observations, the pyrolysis route for DGEBA/DDS has been presented in Scheme 1 (a). With increase in the temperature, the backbone of DGEBA/DDS got broken down. The segments of the bisphenol A and 4, 4′-diaminodiphenyl sulfone were cleaved from the main chain and then pyrolyzed to form numerous low molecular weight aromatic compounds. These low molecular weight aromatic compounds were the major products of the pyrolysis process which were mostly released into the gaseous phase. The release of these compounds in gaseous phase ultimately resulted in formation of low char residues, which was in accordance with TGA results. In the pyrolysis process of DGEM/DDS system, some aromatic components were also released, which were similar to that of DGEBA/DDS system. These aromatic compounds included benzenamine (peak 7), benzenamine, N-methyl- (peak 9), benzenamine, N, N-dimethyl- (peak 10), which indicated that 4, 4′-diaminodiphenyl sulfone segments were cleaved from the main chain and then pyrolyzed to form low molecular aromatic compounds, which then escaped from the system. However, the major pyrolysis peaks of DGEM/DDS system were different from those of DGEBA/DDS, which indicated that its pyrolysis route was different. The major pyrolysis products from DGEM/DDS system were various aliphatic chain products and alicyclic products, which included 5-tridecene, (5E)- (peak 12), spiro [5.5] undec-1-ene (peak 13), 1, 13-tetradecadiene (peak 14), cyclododecene, (Z)- (peak 15), 5-tetradecene, (E)- (peak 16), spiro [5.6] dodecane (peak 17), 1H-fluorene, dodecahydro- (peak 18) and 1-tridecene (peak 19). These products were derived from the random chain degradation of the polyolefin structures in DGEM/DDS system, which were followed by dehydrogenization and cyclization to form the corresponding products. Even so, the total ion peak intensities, especially those for aromatic structures of DGEM/DDS system were much lower than those of DGEBA/DDS system. Considering that equal amount of the two resin samples were used for tests, it was concluded that DGEM/DDS released fewer volatile products during the pyrolysis process and more aromatic components were remained in the condensed phase, which led to its high char yield. Notably, more different kinds of aromatic N-heterocyclic compounds were detected in the pyrolysis process of DGEM/DDS, which included pyridine, 3-methyl- (peak 4), pyridine, 4-methyl- (peak 8), quinoline (peak 11), 2,3,7-trimethylindole (peak 20), 1,6-maphthyridine, 2-methyl- (peak 22), 1H-indole, 1-(phenylmethyl)- (peak 24)

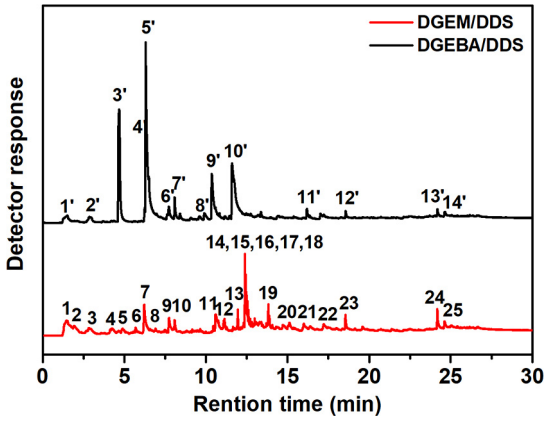

Fig. 13. Total ion chromatograms of Py-GC/MS for DGEM/DDS and DGEBA/DDS.

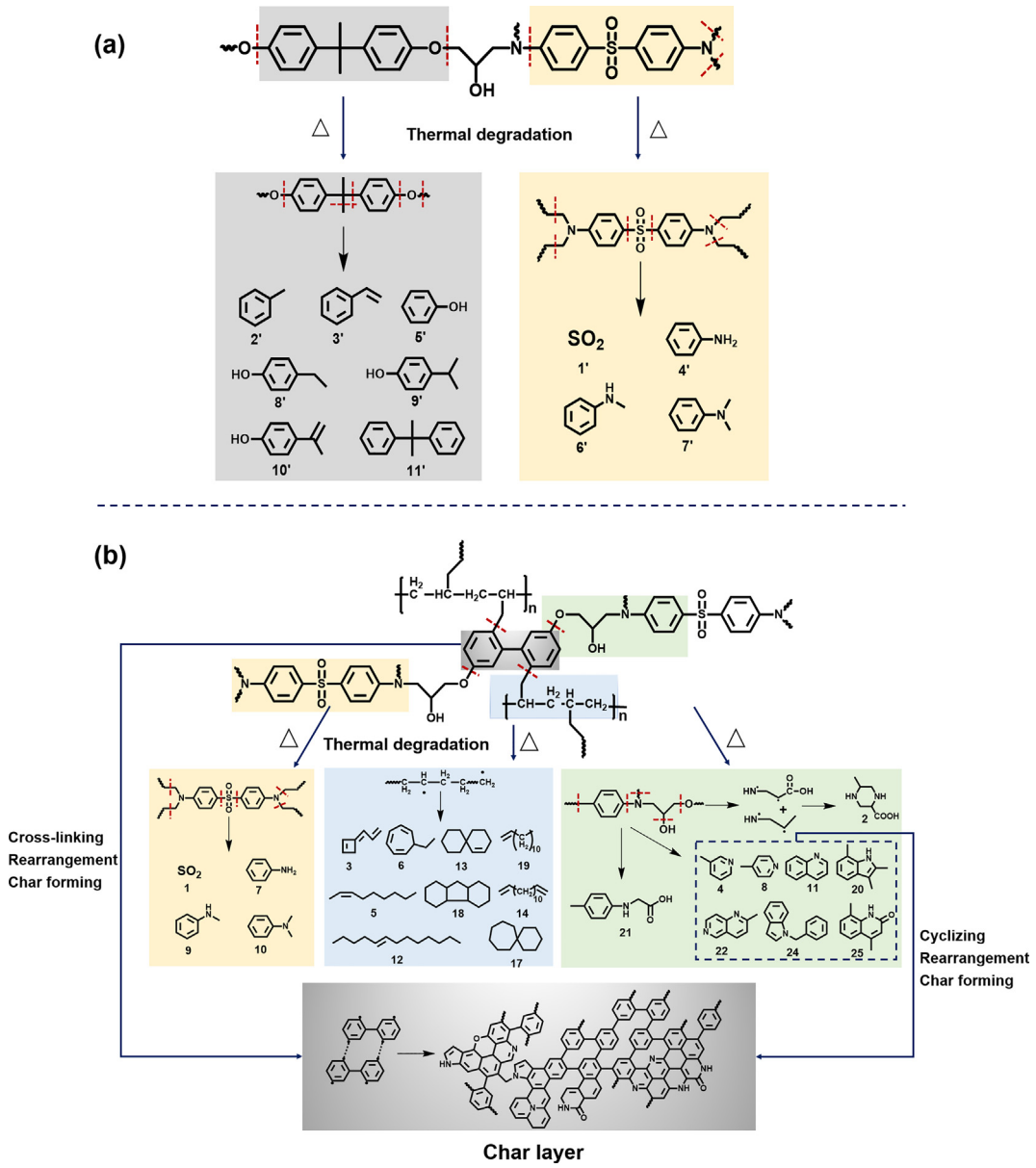

Scheme 1. Proposed pyrolysis routes for (a) DGEBA/DDS; (b) DGEM/DDS.

and 2(1H)-quinolinone, 4,8-dimethyl- (peak 25). These observations suggested that nitrogen presented in DGEM/DDS system was combined with aromatic ring compounds and hydrocarbon chains and then went through cyclization, rearrangement and dehydrogenation reaction and finally produced these aromatic N-heterocyclic compounds. The formation of aromatic N-heterocyclic compounds participated in charring, which enhanced the char residues of this system. In general, more aromatic and aromatic N-heterocyclic structures make contribution to form stable char layers [73]. The probable charring mechanism of DGEM/DDS system has been depicted in Scheme 1(b). When the temperature was increased, the polyolefin and Ar-O bonds were cleaved, which led to the formation the biphenyl radical intermediates. Thereafter, the biphenyl radical intermediates were combined randomly, which underwent cross-linking, arrangement and dehydrogenation reaction. Meanwhile, these biphenyl radical intermediates also reacted with the produced aromatic N-heterocyclic compounds, which finally formed the stable rich aromatic/graphitic char layer containing the pyrrole and pyridine structures. The stable char layer effectively obstructed the heat and flammable gas transfer, and protected the internal resin matrix from further degradation, which endowed the system with higher flame retardancy.

On the basis of analysis results from SEM, XPS, Raman, TG-IR and Py-GC/MS tests, it was concluded that DGEM/DDS exhibited the gaseous phase and condensed phase synergy flame retardant mechanism. In the condensed phase, the presence of the biphenyl structure in DGEM/DDS system effectively enhanced the char yield of this system. Moreover, the production of biphenyl radicals and their reaction to form stable and compact char layer resulted in protection of the inside resins from further degradation. In the gaseous phase, DGEM/DDS system released lots of nonflammable gases, which included CO_2, SO_2 and H_2O. The nonflammable gases took away the heat and diluted the oxygen and other flammable gases. Therefore, the effective synergy of both the gaseous phase and condensed phase made the DGEM/DDS system having better flame retardancy.

4. Conclusion

In this work, a fully bio-based epoxy resin precursor of DGEM was prepared from a biomass raw material of magnolol, through a highly efficient one step process. The special structural characteristics of

magnolol imparted DGEM with a series of excellent properties. With DDS as a curing agent, DGEM/DDS system showed higher curing activity than DGEBA/DDS. After cured, DGEM/DDS revealed an extremely high glass-transition temperature of 279 °C, which is at the highest level among the bio-based epoxy resins reported so far, and much higher than the petroleum-based counterpart of DGEBA/DDS (231 °C). The char yield of DGEM/DDS was as high as 42.8% (in N_2), which is 1.9-fold higher than that of DGEBA/DDS. DGEM/DDS also presented satisfying mechanical properties, with storage modulus of 3678 MPa, and flexural modulus of 3455 MPa. Surprisingly, DGEM possessed an ultra-low viscosity of 0.155 Pa·s at room temperature. Meanwhile, DGEM/DDS system showed a broader processing window than DGEBA/DDS, very suitable for RTM process. Such excellent processability is very rare in the high-performance epoxy resins. Additionally, DGEM/DDS also presented outstanding intrinsic flame retardancy. MCC test signified that DGEM/DDS had shown a 70% and 26% reduction of peak heat release rate and total heat release, respectively, compared to DGEBA/DDS. Furthermore, DGEM/DDS could pass the V-0 rate of the UL-94 test, exerting the gas phase and condensed phase synergy flame retardant mechanism. Thus, magnolol is a fascinating bio-based monomer, which is very suitable to prepare epoxy resins. This work offers an opportunity for the preparation of bio-based epoxy resins substitutable for DGEBA, showing a great potential in cutting-edge areas.

Declaration of Competing Interest

The authors declare that they have no known competing financial interests or personal relationships that could have appeared to influence the work reported in this paper.

Acknowledgements

This work was supported by the National Nature Science Foundation of China (nos. 51873027, U1663226 and 51673033) and the National Key Research and Development Program of China (no. 2017YFB0307600). We also thank Prof. Hongchang Pang in Dalian University of Technology for the assistance with vertical burning test.

Appendix A. Supplementary data

Supplementary data to this article can be found online at https://doi.org/10.1016/j.cej.2020.124115.

References

[1] Y. Zhu, C. Romain, C.K. Williams, Sustainable polymers from renewable resources, Nature 540 (2016) 354–362.
[2] C. Gioia, G. Lo Re, M. Lawoko, L. Berglund, Tunable thermosetting epoxies based on fractionated and well-characterized lignins, J. Am. Chem. Soc. 140 (2018) 4054–4061.
[3] S. Wang, S. Ma, C. Xu, Y. Liu, J. Dai, Z. Wang, X. Liu, J. Chen, X. Shen, J. Wei, J. Zhu, Vanillin-derived high-performance flame retardant epoxy resins: facile synthesis and properties, Macromolecules 50 (2017) 1892–1901.
[4] R. Auvergne, S. Caillol, G. David, B. Boutevin, J.P. Pascault, Biobased thermosetting epoxy: present and future, Chem. Rev. 114 (2014) 1082–1115.
[5] E. Santacesaria, R. Tesser, M. Di Serio, L. Casale, D. Verde, New process for producing epichlorohydrin via glycerol chlorination, Ind. Eng. Chem. Res. 49 (2010) 964–970.
[6] S. Ma, X. Liu, L. Fan, Y. Jiang, L. Cao, Z. Tang, J. Zhu, Synthesis and properties of a bio-based epoxy resin with high epoxy value and low viscosity, ChemSusChem 7 (2014) 555–562.
[7] H. Okada, T. Tokunaga, X. Liu, S. Takayanagi, A. Matsushima, Y. Shimohigashi, Direct evidence revealing structural elements essential for the high binding ability of bisphenol A to human estrogen-related receptor-gamma, Environ. Health. Persp. 116 (2008) 32–38.
[8] R. Steinmetz, N.G. Brown, D.L. Allen, R.M. Bigsby, N. Ben-Jonathan, The environmental estrogen bisphenol A stimulates prolactin release in vitro and in vivo, Endocrinology 138 (1997) 1780–1786.
[9] C. Zhang, T.F. Garrison, S.A. Madbouly, M.R. Kessler, Recent advances in vegetable oil-based polymers and their composites, Prog. Polym. Sci. 71 (2017) 91–143.
[10] J. Chen, X. Nie, Z. Liu, Z. Mi, Y. Zhou, Synthesis and application of polyepoxide cardanol glycidyl ether as biobased polyepoxide reactive diluent for epoxy resin, ACS Sustain. Chem. Eng. 3 (2015) 1164–1171.
[11] P. Jia, M. Zheng, Y. Ma, G. Feng, H. Xia, L. Hu, M. Zhang, Y. Zhou, Clean synthesis of epoxy plasticizer with quaternary ammonium phosphotungstate as catalyst from a byproduct of cashew nut processing, J. Clean. Prod. 206 (2019) 838–849.
[12] M. Chrysanthos, J. Galy, J.P. Pascault, Preparation and properties of bio-based epoxy networks derived from isosorbide diglycidyl ether, Polymer 52 (2011) 3611–3620.
[13] J. Hong, D. Radojčić, M. Ionescu, Z.S. Petrović, E. Eastwood, Advanced materials from corn: isosorbide-based epoxy resins, Polym. Chem. 5 (2014) 5360–5368.
[14] M. Fache, E. Darroman, V. Besse, R. Auvergne, S. Caillol, B. Boutevin, Vanillin, a promising biobased building-block for monomer synthesis, Green Chem. 16 (2014) 1987–1998.
[15] M. Fache, R. Auvergne, B. Boutevin, S. Caillol, New vanillin-derived diepoxy monomers for the synthesis of biobased thermosets, Eur. Polym. J. 67 (2015) 527–538.
[16] G. Yang, B.J. Rohde, H. Tesefay, M.L. Robertson, Biorenewable epoxy resins derived from plant-based phenolic acids, ACS Sustain. Chem. Eng. 4 (2016) 6524–6533.
[17] I. Faye, M. Decostanzi, Y. Ecochard, S. Caillol, Eugenol bio-based epoxy thermosets: from cloves to applied materials, Green Chem. 19 (2017) 5236–5242.
[18] J. Qin, H. Liu, P. Zhang, M. Wolcott, J. Zhang, Use of eugenol and rosin as feedstocks for biobased epoxy resins and study of curing and performance properties, Polym. Int. 63 (2014) 760–765.
[19] S. Wang, S. Ma, Q. Li, X. Xu, B. Wang, W. Yuan, S. Zhou, S. You, J. Zhu, Facile in situ preparation of high-performance epoxy vitrimer from renewable resources and its application in nondestructive recyclable carbon fiber composite, Green Chem. 21 (2019) 1484–1497.
[20] X. Xu, S. Ma, J. Wu, J. Yang, B. Wang, S. Wang, Q. Li, J. Feng, S. You, J. Zhu, High-performance, command-degradable, antibacterial Schiff base epoxy thermosets: synthesis and properties, J. Mater. Chem. A 7 (2019) 15420–15431.
[21] J. Wan, B. Gan, C. Li, J. Molina-Aldareguia, Z. Li, X. Wang, D.Y. Wang, A novel biobased epoxy resin with high mechanical stiffness and low flammability: synthesis, characterization and properties, J. Mater. Chem. A 3 (2015) 21907–21921.
[22] J. Wan, B. Gan, C. Li, J. Molina-Aldareguia, E.N. Kalali, X. Wang, D.Y. Wang, A sustainable, eugenol-derived epoxy resin with high biobased content, modulus, hardness and low flammability: Synthesis, curing kinetics and structure–property relationship, Chem. Eng. J. 284 (2016) 1080–1093.
[23] S. Xu, Y. Han, Y. Guo, Z. Luo, L. Ye, Z. Li, H. Zhou, Y. Zhao, T. Zhao, Allyl phenolic-phthalonitrile resins with tunable properties: Curing, processability and thermal stability, Eur. Polym. J. 95 (2017) 394–405.
[24] B. Yu, W. Xing, W. Guo, S. Qiu, X. Wang, S. Lo, Y. Hu, Thermal exfoliation of hexagonal boron nitride for effective enhancements on thermal stability, flame retardancy and smoke suppression of epoxy resin nanocomposites via sol–gel process, J. Mater. Chem. A 4 (2016) 7330–7340.
[25] N. Amarnath, D. Appavoo, B. Lochab, Eco-friendly halogen-free flame retardant cardanol polyphosphazene polybenzoxazine networks, ACS Sustain. Chem. Eng. 6 (2017) 389–402.
[26] I.D. Carja, D. Serbezeanu, T. Vlad-Bubulac, C. Hamciuc, A. Coroaba, G. Lisa, C.G. López, M.F. Soriano, V.F. Pérez, M.D. Romero, Sánchez, A straightforward, eco-friendly and cost-effective approach towards flame retardant epoxy resins, J. Mater. Chem. A 2 (2014) 16230–16241.
[27] C. Li, H. Fan, T. Aziz, C. Bittencourt, L. Wu, D.Y. Wang, P. Dubois, Biobased epoxy resin with low electrical permissivity and flame retardancy: from environmental friendly high-throughput synthesis to properties, ACS Sustain. Chem. Eng. 6 (2018) 8856–8867.
[28] Z. Li, J. Zhang, F. Dufosse, D.Y. Wang, Ultrafine nickel nanocatalyst-engineering of an organic layered double hydroxide towards a super-efficient fire-safe epoxy resin via interfacial catalysis, J. Mater. Chem. A 6 (2018) 8488–8498.
[29] Y. Feng, J. Hu, Y. Xue, C. He, X. Zhou, X. Xie, Y. Ye, Y.W. Mai, Simultaneous improvement in the flame resistance and thermal conductivity of epoxy/Al_2O_3 composites by incorporating polymeric flame retardant-functionalized graphene, J. Mater. Chem. A 5 (2017) 13544–13556.
[30] L. Chen, C. Ruan, R. Yang, Y.Z. Wang, Phosphorus-containing thermotropic liquid crystalline polymers: a class of efficient polymeric flame retardants, Polym. Chem. 5 (2014) 3737–3749.
[31] E.R. Rad, H. Vahabi, A.R. de Anda, M.R. Saeb, S. Thomas, Bio-epoxy resins with inherent flame retardancy, Prog. Org. Coat. 135 (2019) 608–612.
[32] Y. Qi, J. Wang, Y. Kou, H. Pang, S. Zhang, N. Li, C. Liu, Z. Weng, X. Jian, Synthesis of an aromatic N-heterocycle derived from biomass and its use as a polymer feedstock, Nat. Commun. 10 (2019) 2107.
[33] Y.J. Lee, Y.M. Lee, C.K. Lee, J.K. Jung, S.B. Han, J.T. Hong, Therapeutic applications of compounds in the Magnolia family, Clin. Pharmacol. Ther. 130 (2011) 157–176.
[34] P.K. Mukherjee, N. Maity, N.K. Nema, B.K. Sarkar, Bioactive compounds from natural resources against skin aging, Phytomedicine 19 (2011) 64–73.
[35] R.J. Iredale, C. Ward, I. Hamerton, Modern advances in bismaleimide resin technology: A 21st century perspective on the chemistry of addition polyimides, Prog. Polym. Sci. 69 (2017) 1–21.
[36] D.W.V. Krevelen, Some basic aspects of flame resistance of polymeric materials, Polymer 16 (1975) 615–620.
[37] M. Iji, Y. Kiuchi, Self-extinguishing epoxy molding compound with no flame-retarding additives for electronic components, J. Mater. Sci.-Mater. El. 12 (2001) 715–723.
[38] Q. Luo, M. Liu, Y. Xu, M. Ionescu, Z.S. Petrović, Thermosetting allyl resins derived from soybean oil, Macromolecules 44 (2011) 7149–7157.

[39] M. Xu, Y. Lei, D. Ren, C. Lin, X. Liu, Thermal stability of allyl-functional phthalonitriles-containing benzoxazine/bismaleimide copolymers and their improved mechanical properties, Polymers 10 (2018) 596–611.
[40] K.S. Santhosh Kumar, C.P. Reghunadhan Nair, T.S. Radhakrishnan, K.N. Ninan, Bis allyl benzoxazine: Synthesis, polymerisation and polymer properties, Eur. Polym. J. 43 (2007) 2504–2514.
[41] Y. Luo, M. Xu, H. Pan, K. Jia, X. Liu, Effect of ortho-diallyl bisphenol A on the processability of phthalonitrile-based resin and their fiber-reinforced laminates, Polym. Eng. Sci. 56 (2016) 150–157.
[42] M. Jouyandeh, S.M.R. Paran, A. Jannesari, M.R. Saeb, 'Cure Index' for thermoset composites, Prog. Org. Coat. 127 (2019) 429–434.
[43] M. Jouyandeh, S.M.R. Paran, A. Jannesari, D. Puglia, M.R. Saeb, Protocol for nonisothermal cure analysis of thermoset composites, Prog. Org. Coat. 131 (2019) 333–339.
[44] X. Zou, M. Xu, K. Jia, X. Liu, Synthesis, polymerization, and properties of the allyl-functional phthalonitrile, J. Appl. Polym. Sci. 131 (2014) 1–7.
[45] P.J. Flory, Molecular theory of rubber elasticity, Polymer 20 (1979) 1317–1320.
[46] L.R.G. Treloar, The physics of rubber elasticity, oxford University Press, Oxford, 1975.
[47] J. Wan, J. Zhao, B. Gan, C. Li, J. Molina-Aldareguia, Y. Zhao, Y.T. Pan, D.Y. Wang, Ultrastiff biobased epoxy resin with high Tg and Low permittivity: from synthesis to properties, ACS Sustain. Chem. Eng. 4 (2016) 2869–2880.
[48] S. Zhao, M.M. Abu-Omar, Renewable thermoplastics based on lignin-derived polyphenols, Macromolecules 50 (2017) 3573–3581.
[49] A.S. Mora, R. Tayouo, B. Boutevin, G. David, S. Caillol, Vanillin-derived amines for bio-based thermosets, Green Chem. 20 (2018) 4075–4084.
[50] A. Maiorana, A.F. Reano, R. Centore, M. Grimaldi, P. Balaguer, F. Allais, R.A. Gross, Structure property relationships of biobased n-alkyl bisferulate epoxy resins, Green Chem. 18 (2016) 4961–4973.
[51] M. Janvier, L. Hollande, A.S. Jaufurally, M. Pernes, R. Menard, M. Grimaldi, J. Beaugrand, P. Balaguer, P.H. Ducrot, F. Allais, Syringaresinol: A renewable and safer alternative to bisphenol A for epoxy-amine resins, ChemSusChem 10 (2017) 738–746.
[52] T. Song, Z. Li, J. Liu, S. Yang, Synthesis, characterization and properties of novel crystalline epoxy resin with good melt flowability and flame retardancy based on an asymmetrical biphenyl unit, Polym. Sci. Ser. B 55 (2013) 147–157.
[53] C. Zuo, J. Han, Z. Si, G. Xue, Synthesis, characterization, and properties of a novel epoxy resin containing both binaphthyl and biphenyl moieties, J. Appl. Polym. Sci. 114 (2010) 3889–3895.
[54] N. Teng, S. Yang, J. Dai, S. Wang, J. Zhao, J. Zhu, X. Liu, Making benzoxazine greener and stronger: renewable resource, microwave irradiation, green solvent, and excellent thermal properties, ACS Sustain. Chem. Eng. 7 (2019) 8715–8723.
[55] E. Savonnet, E. Grau, S. Grelier, B. Defoort, H. Cramail, Divanillin-based epoxy precursors as DGEBA substitutes for biobased epoxy thermosets, ACS Sustain. Chem. Eng. 6 (2018) 11008–11017.
[56] J. Dai, Y. Peng, N. Teng, Y. Liu, C. Liu, X. Shen, S. Mahmud, J. Zhu, X. Liu, High-performing and fire-resistant biobased epoxy resin from renewable sources, ACS Sustain. Chem. Eng. 6 (2018) 7589–7599.
[57] T. Liu, C. Hao, S. Zhang, X. Yang, L. Wang, J. Han, Y. Li, J. Xin, J. Zhang, A self-healable high glass transition temperature bioepoxy material based on vitrimer chemistry, Macromolecules 51 (2018) 5577–5585.
[58] D.J. van de Pas, K.M. Torr, Biobased epoxy resins from deconstructed native softwood lignin, Biomacromolecules 18 (2017) 2640–2648.
[59] Y. Jiang, D. Ding, S. Zhao, H. Zhu, H.I. Kenttämaa, M.M. Abu-Omar, Renewable thermoset polymers based on lignin and carbohydrate derived monomers, Green Chem. 20 (2018) 1131–1138.
[60] R. Menard, S. Caillol, F. Allais, Ferulic acid-based renewable esters and amides-containing epoxy thermosets from wheat bran and beetroot pulp: Chemo-enzymatic synthesis and thermo-mechanical properties characterization, Ind. Crop. Prod. 95 (2017) 83–95.
[61] J. Liu, T. Agag, H. Ishida, Main-chain benzoxazine oligomers A new approach for resin transfer moldable neat benzoxazines for high performance applications, Polymer 51 (2010) 5688–5694.
[62] H. Vahabi, B.K. Kandola, M.R. Saeb, Flame Retardancy Index for thermoplastic composites, Polymers 11 (2019) 407–410.
[63] H. Vahabi, F. Laoutid, E. Movahedifar, R. Khalili, N. Rahmati, C. Vagner, M. Cochez, L. Brison, F. Ducos, M.R. Ganjali, M.R. Saeb, Description of complementary actions of mineral and organic additives in thermoplastic polymer composites by Flame Retardancy Index, Polym. Advan. Technol. 30 (2019) 2056–2066.
[64] Y.H. Guan, J.Q. Huang, J.C. Yang, Z.B. Shao, Y.Z. Wang, An effective way To flame-retard biocomposite with ethanolamine modified ammonium polyphosphate and its flame retardant mechanisms, Ind. Eng. Chem. Res. 54 (2015) 3524–3531.
[65] X. Dong, L. Chen, R.T. Duan, Y.Z. Wang, Phenylmaleimide-containing PET-based copolyester: cross-linking from $2\pi + \pi$ cycloaddition toward flame retardance and anti-dripping, Polym. Chem. 7 (2016) 2698–2708.
[66] Y. Tan, Z.B. Shao, L.X. Yu, J.W. Long, M. Qi, L. Chen, Y.Z. Wang, Piperazine-modified ammonium polyphosphate as monocomponent flame-retardant hardener for epoxy resin: flame retardance, curing behavior and mechanical property, Polym. Chem. 7 (2016) 3003–3012.
[67] J.N. Wu, L. Chen, T. Fu, H.B. Zhao, D.M. Guo, X.L. Wang, Y.Z. Wang, New application for aromatic Schiff base: High efficient flame-retardant and anti-dripping action for polyesters, Chem. Eng. J. 336 (2018) 622–632.
[68] J.R. Pels, F. Kapteijn, J.A. Moulijn, Q. Zhu, K.M. Thomas, Evolution of nitrogen functionalities in carbonaceous materials during pyrolysis, Carbon 33 (1995) 1641–1653.
[69] H. Duan, Y. Chen, S. Ji, R. Hu, H. Ma, A novel phosphorus/nitrogen-containing polycarboxylic acid endowing epoxy resin with excellent flame retardance and mechanical properties, Chem. Eng. J. 375 (2019) 121916.
[70] W.J. Liang, B. Zhao, P.H. Zhao, C.Y. Zhang, Y.Q. Liu, Bisphenol-S bridged penta (anilino)cyclotriphosphazene and its application in epoxy resins: Synthesis, thermal degradation, and flame retardancy, Polym. Degrad. Stabil. 135 (2017) 140–151.
[71] J.T. Miao, L. Yuan, Q. Guan, G. Liang, A. Gu, Biobased heat resistant epoxy resin with extremely high biomass content from 2,5-furandicarboxylic acid and eugenol, ACS Sustain. Chem. Eng. 5 (2017) 7003–7011.
[72] H. Chen, J. Wang, A. Ni, A. Ding, X. Han, Z. Sun, The effects of a macromolecular charring agent with gas phase and condense phase synergistic flame retardant capability on the properties of PP/IFR composites, Materials 11 (2018) 111.
[73] D.J. Liao, Q.K. Xu, R.W. McCabe, H.V. Babu, X.P. Hu, N. Pan, D.Y. Wang, T.R. Hull, Ferrocene-based nonphosphorus copolymer: Synthesis, high-charring mechanism, and its application in fire retardant epoxy resin, Ind. Eng. Chem. Res. 56 (2017) 12630–12643.